



## ORIGINAL ARTICLE

# Experimental and DFT evaluation of adsorption and inhibitive properties of *Moringa oleifera* extract on mild steel corrosion in acidic media

Christogonus Oudney Akalezi<sup>a,c,\*</sup>, Arinze Chidiebere Maduabuchi<sup>b</sup>,  
Conrad Kenekwue Enenebeaku<sup>a</sup>, Emeka Emmanuel Oguzie<sup>a,c</sup>

<sup>a</sup> Department of Chemistry, School of Physical Sciences, Federal University of Technology, Owerri, Nigeria

<sup>b</sup> Department of Science Laboratory Technology, School of Physical Sciences, Federal University of Technology, Owerri, Nigeria

<sup>c</sup> African Center of Excellence in Future Energies and Electrochemical Systems (ACE-FUELS), Federal University of Technology, Owerri, Nigeria

Received 29 August 2020; accepted 1 November 2020

Available online 10 November 2020

## KEYWORDS

*Moringa oleifera*;  
Plant extract;  
Inhibitor;  
Experimental technique;  
DFT technique

**Abstract** The corrosion response of mild steel in 0.5 M H<sub>2</sub>SO<sub>4</sub> acid solution in the presence of *Moringa oleifera* (MO) leaf extract was investigated using gravimetric, electrochemical, and DFT techniques. Gravimetric results indicate that MO exhibits a high inhibition value up to 93.0% when the concentration was 1.5 g/L. Inhibition value in general increased with an increase in concentration of the extracts but decreased with prolonged exposure time and temperature. Analysis of polarization curves indicated that MO extract acted as mixed-type inhibitors. The adsorption process of MO on a mild steel surface in the acid solution fitted the Langmuir isotherm. GC/MS analysis of MO extract revealed the presence of more than 29 active constituents including 9,12-Octadecadienoic acid (Z, Z) methyl ester (28.55%); n-Hexadecanoic acid (11.24%); 9,12,15-Octadecatrienoic acid methyl ester (9.31%), Benzeneacetonitrile, 4-hydroxy-(6.32%), 2-Furancarboxaldehyde,5-(hydroxymethyl)- (5.6%), Heptadecane (4.85%). Quantum chemical calculations were applied on some of the identified constituents to assess their adsorbability on the mild steel surface and the result revealed remarkable high interaction energies.

© 2020 Published by Elsevier B.V. on behalf of King Saud University. This is an open access article under the CC BY-NC-ND license (<http://creativecommons.org/licenses/by-nc-nd/4.0/>).

\* Corresponding author at: Department of Chemistry, School of Physical Sciences, Federal University of Technology, Owerri, Nigeria.  
E-mail addresses: [christogonus.akalezi@futo.edu.ng](mailto:christogonus.akalezi@futo.edu.ng) (C.O. Akalezi), [oguziemeka@gmail.com](mailto:oguziemeka@gmail.com) (E.E. Oguzie).  
Peer review under responsibility of King Saud University.



Production and hosting by Elsevier

## 1. Introduction

Mild steel is widely used in the industries, especially in the construction, metal extraction, oil drilling, and processing and distribution industries as holding tanks, boilers and pipe lines. Different commercial organic and inorganic acids are used during industrial cleaning and pretreatment processes, oil well acidizing, acid pickling, and descaling, and these

operations engender large scale acid consumption and material wasting (Abdel Gaber et al., 2020; Nahle et al., 2018). The use of corrosion inhibitors is the most viable alternative to reduce corrosion damage and hence prolong the life span of these service/structural materials (Sastri, 1998a, 1998b). Some of the most effective corrosion inhibitors in used today are organic compounds containing heteroatoms such as O, N, and S and multiple bonds in their structures (Thirumalairaj et al., 2016; Goulart et al., 2013; Benali et al., 2007). The special character of these compounds is their ability to coordinate with the dissolving metal substrates through the formation of protective layers on the metal surfaces (Shalabi et al., 2014; Bhawsar et al., 2015). At present several organic inhibitors belonging to different chemical families such as fatty amides (Olivares-Xometl et al., 2006; Olivares-Xometl et al., 2008), pyridines (Abd El-Maksoud et al., 2005; Ergun et al., 2008; Noor, 2009), imidazolines (Cruz et al., 2004; Liu et al., 2009; Martinez-Palou et al., 2004; Olivares-Xometl et al., 2006, 2009) and other azoles (Likhanova et al., 2007; Popova et al., 2007; Antonijevic et al., 2009), all with excellent performance as corrosion inhibitors (RSC, 1990). However, despite their good performance, the use of these synthetic organic corrosion inhibitors is now being regulated. A good number of these corrosion inhibitors are hazardous to human health and the environment as well. Much attention is now being devoted to the development of organic compounds of plant origin whose constituents such as tannins, organic and amino acids, alkaloids, and pigments are known to exhibit inhibiting action against corrosion damage (Singh et al., 2012). Many plant materials have been successfully investigated and confirmed as potential corrosion inhibitors of acid corrosion of metals including, *Lawsonia* (El-Etre, 2005), *Dacryodis edulis* (Oguzie et al., 2012), *Medicago Sativa* (Al-Turkustani et al., 2011) *Azadirachta indica* (Bothi and Mathur, 2009), *Solanum tuberosum* (Okafor et al., 2010), to name a few.

*Moringa oleifera* Lam syn; a monogeneric family of *Moringa* is one of those plants in which all the parts are considered useful (leave, flowers, roots, and fruits) due to their various medicinal and nutritive values (Nadkarni, 2009; Ramachandran et al., 1980). *Moringa* leaves in particular exhibit good antioxidant properties due to the presence of various compounds such as ascorbic acid flavonoids, phenolics, carotenoids, etc. (Arabshahi et al., 2007). *Moringa oleifera*, initially native to sub-Himalayan tracts of India, Pakistan, Bangladesh, and Afghanistan is now widely distributed and naturalized in many parts of African including Nigeria (Singh et al., 2012a). The use of *Moringa oleifera* as a potential additive for mitigation of mild steel corrosion in acidic environment has received some attention (Jalajaa et al., 2019; Allaoui et al., 2017; Anwar and Bhang, 2003).

The present study investigates the inhibitive action and adsorption behavior of MO during mild steel corrosion in 0.5 M H<sub>2</sub>SO<sub>4</sub> utilizing gravimetric and electrochemical techniques. The study will be extended to identify the compounds available in the leaf extract which are responsible for its inhibition action towards mild steel corrosion in acidic media. Also, some of the identified compounds will be modeled and analyzed using the DFT approach to shed more light on the mechanism and adsorption properties of this additive.

## 2. Experimental

### 2.1. Materials preparation

A bulk metal sheet of the following composition was obtained for this study: C (0.01%), Mn (0.34%), P (0.08%), and Fe (99.51%). For the gravimetric measurements, coupons of dimension 3 cm × 3 cm × 0.1 cm were obtained. These coupons were used as procured without further polishing but were degreased in absolute ethanol, dried in acetone before use. Test metal samples for electrochemical experiments were cut into dimensions such that only a 1 cm<sup>2</sup> contact area was left uncovered after sealing with epoxy resin. The exposed surfaces were then polished with emery papers (800 to 1200 grits) successively, rinsed with distilled water, degreased with ethanol, dried in acetone before use. All reagents were BDH analytical grade and used as sourced without further purification. Distilled water was used for all solutions preparations. 0.5 M H<sub>2</sub>SO<sub>4</sub> solutions were employed as the aggressive medium.

Ethanollic *MO* leaf extract stock solution was obtained using the same procedure reported previously (Akalezi et al., 2016a, 2016b). About 100 g of sun-dried powdered *MO* leaves was taken in a Soxhlet extractor with 400 mL ethanol and continuously refluxed for 6 h. The solution was allowed to cool and then filtered using Whatman No.1 filter paper. The filtrate was concentrated by evaporating the solvent to dryness on a water bath to obtain a gel. The weight of the extract is taken and kept at 4 °C before use. From the crude extract, various inhibitor concentrations ranging from 0.1 g/L to 1.5 g/L were prepared and used to evaluate the corrosion inhibition efficacy.

### 2.2. Gravimetric measurements

During the gravimetric experiment, the mild steel samples were weighed accurately (using a FAJA weighing balance of range 0.0001 to –200 g) and then immersed in 200 mL test solutions at 303 K. The test coupons were retrieved (at 24 h intervals up to 120 h), scrubbed with bristle brush under running water, dried, and reweighed. Tests were also conducted at 313 K, 323 K, and 333 K temperatures respectively, but this time the coupons were retrieved after 3 h duration. All tests were conducted in aerated and unstirred test solution. The corrosion rate (CR), and inhibition efficiency (IE%) were determined using the following equations:

$$CR = \frac{w_o - w_i}{AT} \quad (1)$$

$$\theta = \frac{w_o - w_i}{w_o} \quad (2)$$

$$IE\% = \theta \times 100 \quad (3)$$

where CR is the average corrosion rate in milligrams per square decimeter per day (mdd);  $w_i$  and  $w_o$  are the weight loss values (in mg) in presence and absence of inhibitor, respectively; A is the initial exposed area of coupon, square decimeters (0.1911 dm<sup>2</sup>); T is the exposure time, (in days). The weight loss reported is the average of three replicate measurements.

### 2.3. Electrochemical measurements

#### 2.3.1. Potentiodynamic polarization (PDP) experiments

Potentiodynamic polarization experiments were conducted in a three-electrode corrosion cell using a Princeton Applied Research (PAR) corrosion system, (Model 263), with power suite software.

A graphite rod was used as a counter electrode and a saturated calomel electrode (SCE) was used as a reference electrode. The latter was connected via a luggin capillary. Mild steel coupons serve as a working electrode. Measurements were performed in aerated and unstirred solutions at the end of 24 h of immersion at open circuit potential ( $E_{OCP}$ ) at 303 K. Tafel curves were obtained by scanning the electrode potential from  $-250$  to  $+250$  mV versus corrosion potential ( $E_{corr}$ ) at a sweep rate of  $0.5 \text{ mVs}^{-1}$ . The linear Tafel segments of anodic and cathodic curves were extrapolated to obtain corrosion current densities ( $I_{corr}$ ). The inhibition efficiency was evaluated from the measured  $I_{corr}$  values using the relationship:

$$\eta_{pdp} \% = \frac{I_{corr}^0 - I_{corr}}{I_{corr}^0} \times 100\% \quad (4)$$

where  $I_{corr}^0$  and  $I_{corr}$  are the corrosion current densities in absence and in presence of inhibitor, respectively.

#### 2.3.2. Electrochemical impedance spectroscopy (EIS) experiments

EIS tests were performed using VersaSTAT3 Potentiostat/Galvanostat in an interval between 10 MHz and 100 kHz at an excitation voltage of 10 mV. A graphite electrode and saturated calomel electrodes (SCE) were the auxiliary and reference electrodes, respectively. The working electrode was immersed in a test solution for 24 h at open circuit potential ( $E_{OCP}$ ) at 303 K, sufficient to attain a stable state. The electrochemical data was analyzed using the ZsimpWin impedance modeling package. The inhibition value  $\eta_{EIS}$  (%) was gotten from the charge transfer resistance ( $R_{ct}$ ) as follows:

$$\eta_{EIS} \% = \frac{R_{ct} - R_{ct}^0}{R_{ct}} \times 100 \quad (5)$$

where  $R_{ct}^0$  and  $R_{ct}$  are charge transfer resistance for mild steel in  $0.5 \text{ M H}_2\text{SO}_4$  without and with inhibitor. The data recorded were averages of three replicate measurements.

### 2.4. Surface examination studies

The mild steel was immersed in  $0.5 \text{ M H}_2\text{SO}_4$  solution for 24 h at 303 K in the absence and presence of  $1.5 \text{ g/L}$  concentration of MO extract. The mild steel specimens were taken out, washed with double distilled water, dried, and finally analyzed by SEM instrument, a Shimadzu SSX-550 at an accelerating voltage of 5 kV and  $\times 2000$  magnification.

### 2.5. Fourier transform infrared spectroscopic analysis of MO leaf extract

The MO leaf extract was examined under Fourier transform infrared (FTIR) spectroscopic analysis using a Nicolet-Magma-IR 560 (KBr pellet) in the  $4500\text{--}500 \text{ cm}^{-1}$  interval,

and the peak values recorded. Each analysis was twice repeated to detect the characteristic peaks and their functional groups.

### 2.6. Gas chromatography - mass spectrometry (GC/MS) analysis

The Moringa oliefera leaf extract was also analyzed on a GC-MS Agilent Tech GC/MS (Model 5975C) equipped with a DB-5 ms fused silica capillary column ( $30 \times 0.25 \text{ mm ID}$ ; film thickness:  $0.25 \mu\text{m}$ ), operating in electron impact mode at 70 eV. Pure helium (99.999%) was used as carrier gas at a constant flow of  $1.6 \text{ mL/min}$ ; an injection volume of  $5 \mu\text{L}$  was employed at split ratio is 10: 1. Mass transfer line and injector temperature were set at 230 and 250 °C, respectively. The oven temperature was programmed from 70 (isothermal for 3 min) to 300 °C (isothermal for 9 min) at the rate of  $10 \text{ }^\circ\text{C/min}$ . Total GC running time was 50 min.

### 2.7. Quantum chemical computations

One of the major flaws with plant extracts inhibition studies is the limited information on the mechanism of inhibition given the complex chemical composition. Density functional theory (DFT) was adopted to precisely obtain information about molecular geometric and electron distribution. This approach has been widely used for analysis of inhibitor efficiency and inhibitor-surface interaction. In this study, the geometric configuration of the molecules involved were optimized with Materials studio 4.0 software (Accelrys, Inc.) and the frequency analysis was performed to ensure that the researched molecules reached their respective ground state.

### 2.8. Molecular dynamics simulation

The interaction of inhibitor molecules with the metal surface was investigated with molecular dynamics (MD) simulation. An adsorption model containing one inhibitor molecule and metallic surface was built using a Forcite quench module in the Materials Studio (Model 4.0) software. The simulation system was optimized with the COMPASS force field (Zhang et al., 2010). The Fe crystal was cleaved along the (1 1 0) plane with a fractional depth of 3.0. The geometry of the bottom layers is constrained before optimizing the Fe(1 1 0) surface, which was subsequently enlarged into an  $8 \times 8$  supercell. The temperature was fixed at 350 K which represents a tradeoff between a system with too much kinetic energy, where the molecules desorb from the surface, and a system with not enough kinetic energy for the molecule to move around the surface. The simulation time was 500 ps at a time step of 1 fs, and a frame was recorded every 250 steps during simulation. The binding energy of molecules on the metal surface (denoted as  $E_{bind}$ ) was calculated as follows:

$$E_{bind} = (E_{molecule} + E_{surface}) - E_{total} \quad (6)$$

In above equation,  $E_{molecule}$ ,  $E_{surface}$ , and  $E_{total}$  represent the energy of single molecule, metal surface without adsorption, and total system containing a molecule and metal surface, respectively.

### 3. Results and discussion

#### 3.1. Gravimetric experiment

##### 3.1.1. The impact of time and concentration

Table 1 displays the gravimetric corrosion parameters during mild steel corrosion in 0.5 M H<sub>2</sub>SO<sub>4</sub> at 303 K in the absence and presence of different concentration of MO leaf extract. Inspection of the data reveals an ascending order in the inhibition efficiency up to 92.63% at 1.5 g/L concentration. There was no further increase beyond this concentration. The increasing inhibition efficiency suggests improvement in surface coverage with increasing concentration of inhibitor. This outcome is likely due to the adsorption of MO extract constituents onto the mild steel surface and subsequent formation of a shielding physical barrier to reduce the acid attack (Abdu and Sathiq, 2016), with a corresponding decrease in weight loss and corrosion rate, respectively.

Fig. 1 represents the impact of extended immersion time on the inhibition efficiency of MO extract at the optimum concentration, as extracted from Table 1. The data presented shows that the IE% increase during the initial 72 h, and then a decrease followed. The increase in efficiency with time can be correlated with film growth and rearrangement of the inhibitor molecules on mild steel surface (Singh et al., 2012b), while the decrease is the desorption of adsorbed extract components on the mild steel surface (Abdallah, 2002).

##### 3.1.2. Effect of temperature

The effect of temperature on the inhibited solution-metal reaction is highly complex, because many changes occur on the metal surface such as rapid etching, in acidic solution, desorption of inhibitor and the inhibitor itself may undergo decomposition and/or molecular rearrangement (Noor, 2007).

As observed from the data in Table 2, the corrosion rate increased with increasing temperature, both in uninhibited and inhibited solutions. Inhibiting potency was also present, as evident in Fig. 2., even though the values were decreasing with temperature rise. Kumar et al (2013) found that the protection efficiency of *Achyranthes Aspera* extracts decreases with increasing temperature from 303 K to 333 K. They attributed this behaviour to increased rate of dissolution process of mild steel and partial desorption of the inhibitor from the metal surface with temperature. The decrease in the strength

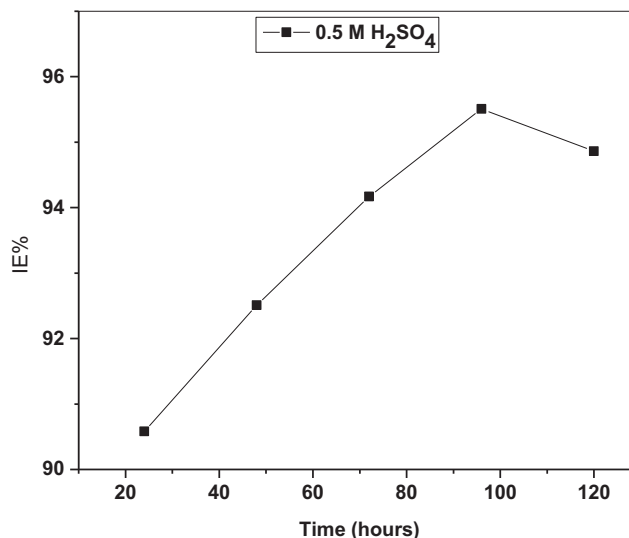


Fig. 1 Effect of time on the inhibition efficiency of MO leaf extract during corrosion of mild steel in 0.5 M H<sub>2</sub>SO<sub>4</sub> at 303 K.

Table 2 Corrosion parameters at different temperatures (303 to 333 K) for mild steel corrosion without and containing 1.5 g/L MO leaves extract.

Temp. (K)	CR (mdd) (Blank)	CR(mdd) (inhibited)	IE%
303	562.43	41.72	92.63
313	928.31	157.51	83.03
323	1377.29	234.43	82.98
333	1658.82	341.18	79.43
Ea (kJ/mole)	13.13	25.51	

of adsorption process at higher temperatures, may be a clear lead to the dominating mechanism of adsorption, which may be of the physical type.

To further obtain the activation parameters for this corrosion system, the modified form of the Arrhenius equation was applied (Akalezi & Oguzie, 2016):

$$\log\left(\frac{CR_2}{CR_1}\right) = + \frac{E_a}{R} \left(\frac{1}{T_1} - \frac{1}{T_2}\right) \tag{7}$$

Table 1 Effect of time and concentration of inhibitor on corrosion of mild steel in 0.5 M H<sub>2</sub>SO<sub>4</sub> at 303 K from gravimetric technique.

Concentration (g/L)	Time (hours)					
	Parameters	24	48	72	98	120
0.5M H <sub>2</sub> SO <sub>4</sub>	Δw (g)	1.0748	1.7642	2.0788	2.1716	2.2756
	CR (mdd)	5.6243	18.4636	32.6342	45.4547	59.5395
0.1	Δw (g)	0.5901	0.9133	1.0531	1.1473	1.2263
	IE(%)	45.10	48.22	49.34	47.85	46.11
0.5	Δw (g)	0.1587	0.2337	0.3074	0.3849	0.4933
	IE(%)	85.22	86.75	85.21	82.27	78.32
1.0	Δw (g)	0.1099	0.1414	0.1546	0.2602	0.2720
	IE(%)	89.77	91.98	92.56	88.01	88.04
1.5	Δw (g)	0.0690	0.0770	0.0825	0.0975	0.1624
	CR (mdd)	0.3610	0.80586	1.2951	2.048	4.2491
	IE(%)	93.58	95.63	96.03	95.51	92.86

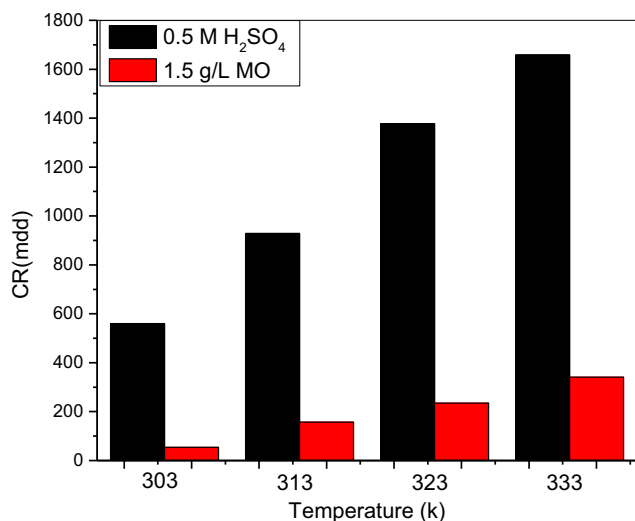


**Fig. 2** Effect of temperature during the corrosion of mild steel in 0.5 M H<sub>2</sub>SO<sub>4</sub> in the absence and containing 1.5 g/L MO leaf extract.

where  $E_a$  is the apparent activation energy,  $R$  is the universal gas constant ( $\text{Jmol}^{-1} \text{K}^{-1}$ ),  $CR_1$  and  $CR_2$  are the corrosion rates at the temperatures  $T_1$  and  $T_2$  respectively (in this case 303 and 333 K). Table 4 lists some of corrosion parameters at different temperatures (303 to 333 K). It is obvious that  $E_a$  values (Table 2) for the mild steel dissolution in 0.5 M H<sub>2</sub>SO<sub>4</sub> solution containing 1.5 g/L MO leaf extract were higher than that in the uninhibited which scenario is widely accepted as evidence of physisorption mechanism (Popova et al., 2003; Szauer, 1981).

### 3.2. Adsorption isotherm

MO extract molecules adsorbing on the metal surface and the interactions between metal–inhibitor at the interface was explained through adsorption isotherms. Several adsorption isotherms were tried to fit the weight loss

values to get a linear fit. However, adsorption of molecules followed the Langmuir adsorption isotherm. Surface coverage ( $\theta$ ) is linked with the adsorbate in the bulk of electrolyte  $C_{inh}$  as in the following equations (Singh et al., 2017; Tan et al., 2020; Vasudha et al., 2012; Martinez, 2003).

$$\theta = \frac{K_{ads}C_{inh}}{1 + K_{ads}C_{inh}} \quad (8a)$$

where  $K_{ads}$  is the equilibrium constant for the adsorption/ desorption process. The equation can be rewritten as:

$$\frac{C_{inh}}{\theta} = \frac{1}{K_{ads}} + C_{inh} \quad (8b)$$

A plot between  $C_{inh}/\theta$  versus  $C_{inh}$  (Fig. 3) gave linear-fit plots of MO extract with the correlation coefficient ( $R^2$ ) of 0.9987 with a slope 1.020. The unity slope obtained, from the plot suggests that the adsorbed inhibitor molecules form monolayer on the mild steel surface and there is no interaction among the adsorbed inhibitor molecules (El-Haddad et al., 2015). The equilibrium adsorption constant ( $K_{ads}$ ) was not calculated because the specific molecular mass of the extract constituents could not be determine.

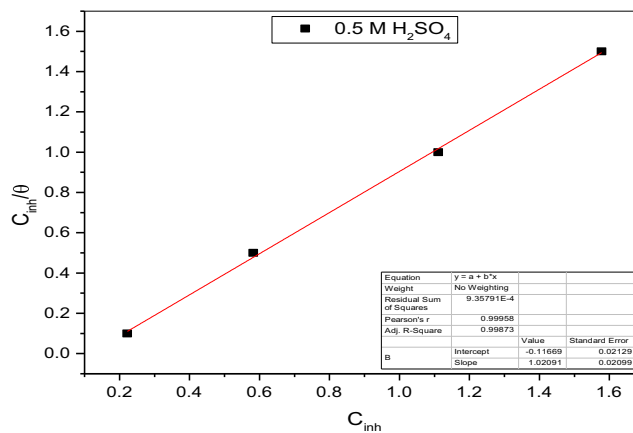


**Fig. 3** Langmuir isotherm for adsorption of MO extract on mild steel in 0.5 M H<sub>2</sub>SO<sub>4</sub> at 303 K.

### 3.3. Electrochemical results

#### 3.3.1. Potentiodynamic polarization (PDP) results

Fig. 4 shows the polarization curves for mild steel in 0.5 M H<sub>2</sub>SO<sub>4</sub> solution containing 1.5 g/L MO extracted from different water and ethanol solvents. Table 3 displays the PDP parameters obtained; the corrosion potential ( $E_{corr}$ ), corrosion current density ( $i_{corr}$ ), cathodic and anodic Tafel slopes ( $\beta_c$  and  $\beta_a$ ), and inhibition efficiency ( $\eta_{pdp}$  %). As evident from Fig. 4, the addition of the extract decreased the current densities of both the anodic and cathodic branches indicating that both the anodic and cathodic reaction rates were suppressed. It is also noticeable that the shape of the PDP curves did not change with the addition of MO extract implying no change the corrosion mechanism following the addition (Satapathy et al., 2009). Therefore, the inhibitive effect of this additive originates from the coverage of the extract mass on the metal surface thus preventing its exposure to the acidic environment. According to corrosion theory (Jones, 1983), the slight rightward of the inhibited towards the more negative potential revealed that MO extracts were of mixed type inhibitors, but predominantly cathodic (Abd-El Rehim et al., 2001; Issaadi et al., 2011; Li et al., 2011). The solvents used to obtain the extract (water and ethanol) gave almost identical results as displayed in Table 3.

#### 3.3.2. Electrochemical impedance (EIS) results

The representative EIS plot in Nyquist format for mild steel dissolution in 0.5 M H<sub>2</sub>SO<sub>4</sub> solution at 303 K in the absence and presence of 1.5 g/l MO extract obtained from ethanol and water solvents respectively are shown in Fig. 5. Furthermore, Bode plots can give more information in case of more intricate systems. The Bode plots of the synthesized inhibitors are presented in Fig. 6. It is obvious from Figs. 5 and 6, that the diameter of the capacitive loops became larger with the addition of the extract than that in its absence, suggesting that the mild steel dissolution process was remarkably restrained by this additive. As observed, for both the inhibited as well as the uninhibited cases, the impedance spectrum contains only one depressed capacitive loop, characteristic of a single “time constant” which was represented by the electrochemical equivalent circuit shown in Fig. 7. This finding is consistent with previ-

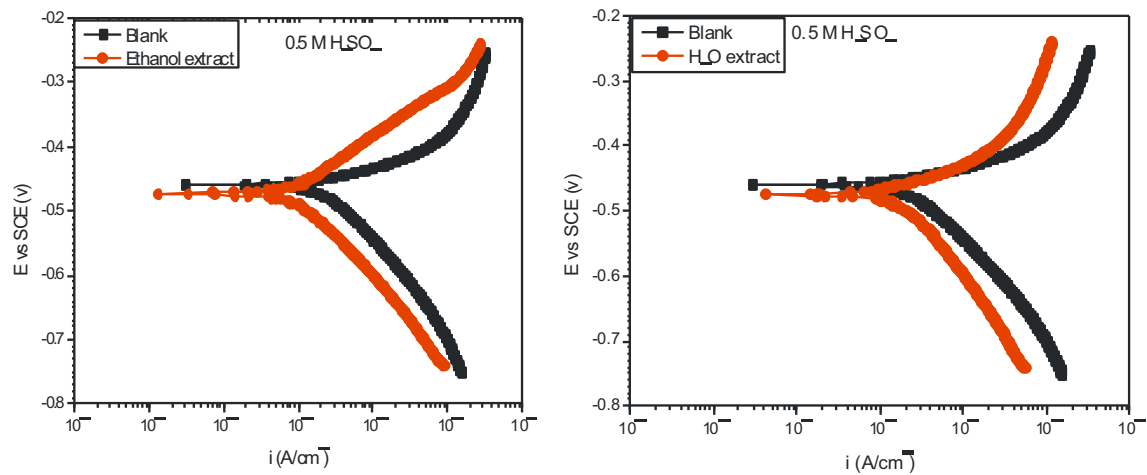


**Fig. 4** Potentiodynamic polarization curves of mild steel in 0.5 M  $\text{H}_2\text{SO}_4$  solution without and with 1.5 g/L ethanol extract of M.O at 303 K.

**Table 3** Polarization parameters for mild steel corrosion in 0.5 M  $\text{H}_2\text{SO}_4$  in absence and presence of 1.5 g/L of different extracts (ethanol and water) of MO.

System	$E_{\text{corr}}$ (mV)	$I_{\text{corr}}$ $\mu\text{A}/\text{cm}^2$	$B_c$ mV	$B_a$ mV	$E_p\%$
Blank 0.5 M $\text{H}_2\text{SO}_4$	-460	58.4	98	33	–
Ethanol Extract M.O (1.5 g/L)	-474	19.8	126	90	66.0.09
Water Extract M.O (1.5 g/L)	-464	20.4	119	44	65.07

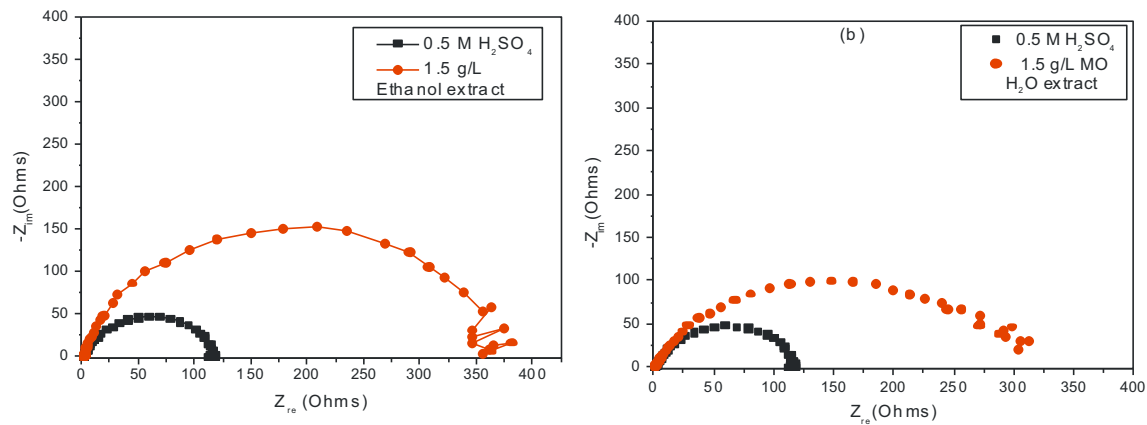


**Fig. 5** Nyquist plots for mild steel corrosion in 0.5 M  $\text{H}_2\text{SO}_4$  solution at 303 K containing 1.5 g/L concentrations of MO extract from (a) ethanol solvent and (b) from water.

ously published equivalent circuits (Khaled, 2003; Morad, 2000; Roque et al., 2008), indicating a non-ideal electrochemical behavior at the metal/solution interface (Hosseini et al., 2003; Khaled et al., 2004). Such a result is generally attributed to heterogeneities or non-homogeneities of the metal surface (Solmaz et al., 2008; Nam et al., 2013). Therefore, to obtain an improved fit of the experimental data set, a constant phase element (CPE) was used in place of the capacitance (Nam et al., 2013). The admittance of a CPE can be calculated using the following expression (Hussin et al., 2016):

$$\frac{1}{Z_{\text{cpe}}} = Y(\text{cpe}) = Y_0(j\omega)^n \quad (9)$$

where  $Y_0$  is the magnitude,  $j$  equals  $-1$ ,  $\omega$  is the angular frequency, and  $n$  is the phase shift, representing the surface inhomogeneity. The double-layer capacitance ( $C_{dl}$ ) were determined according to the relations given below (Das et al., 2017; Zarrouk et al., 2015):

$$C_{dl} = Y_0^{1/n} + R_{ct}^{(1-n)/n} \quad (10)$$

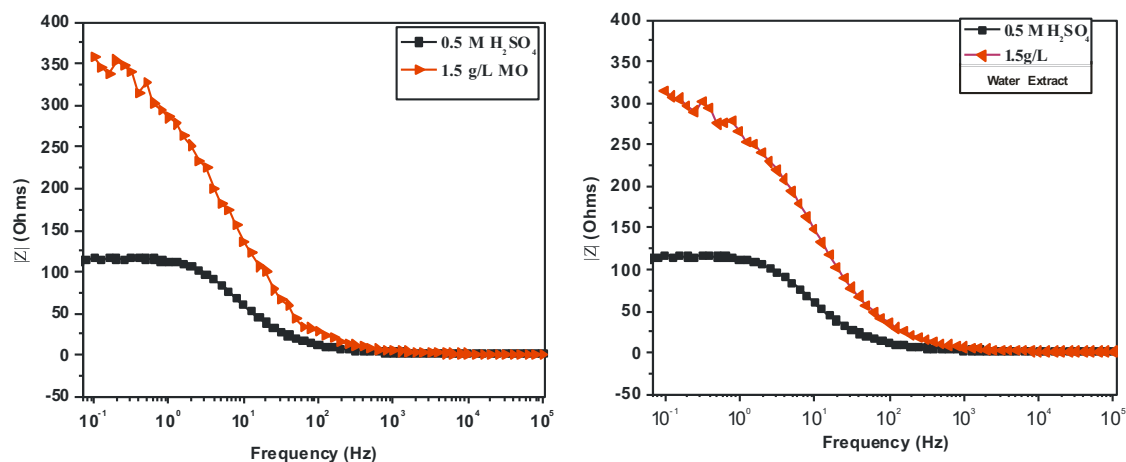


Fig. 6 Bode plot of mild steel in 0.5 M  $\text{H}_2\text{SO}_4$  without and with 1.5 g/L concentrations of MO extract.

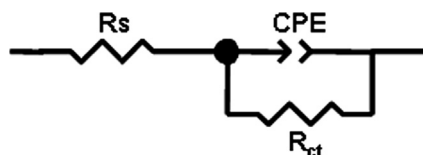


Fig. 7 Electrochemical Equivalent Circuit model used to simulate the EIS data ( $R_s$ : solution resistance, CPE: constant phase element (CPE);  $R_{ct}$ : charge transfer resistance).

where  $Y_0$  and  $n$  are magnitudes of CPE and deviation parameter ( $-1 \leq n \leq 1$ , which is dependent on surface morphology).

The  $C_{dl}$  values, generally, are inversely proportional to the adsorbent concentration on the metal surface.

The fitted results are summarized in Table 4. It can be seen that the values of  $R_{ct}$  increased upon the addition of inhibitor, suggesting a higher corrosion resistance by the adsorption of these inhibitors onto mild steel surface.

### 3.4. Surface examination

SEM image of mild steel samples after being corroded in 0.5 M  $\text{H}_2\text{SO}_4$  solution without and with addition of 1.5 g/L of MO extract is shown in Fig. 8. It is observed that the mild steel surface was strongly damaged without inhibitors (Fig. 8a), but the surface was smoothed when 1.5 g/L inhibitors was added (Fig. 8b), indicating that MO extract formed a protective physical barrier on the mild steel surface and suppressed the acid aggression (see Fig. 9).

The presence of these inhibitors was further confirmed by FTIR spectra, as shown in Fig. 8. From FTIR spectra of the extract only two peaks appeared which were not seen in the spectra of the pure extract in the acids. These peaks are at  $2975 \text{ cm}^{-1}$  attributed to the stretching mode for aliphatic and aromatic C-H groups and at  $2350 \text{ cm}^{-1}$ . All other peaks in powder appear in the spectra for the extract in acids. Thus these two peaks must be significant in the formation of the protective film by donation of  $n$  and  $\pi$  electrons to the metal.

### 3.5. GC-MS characterization of the ethanol extract MO

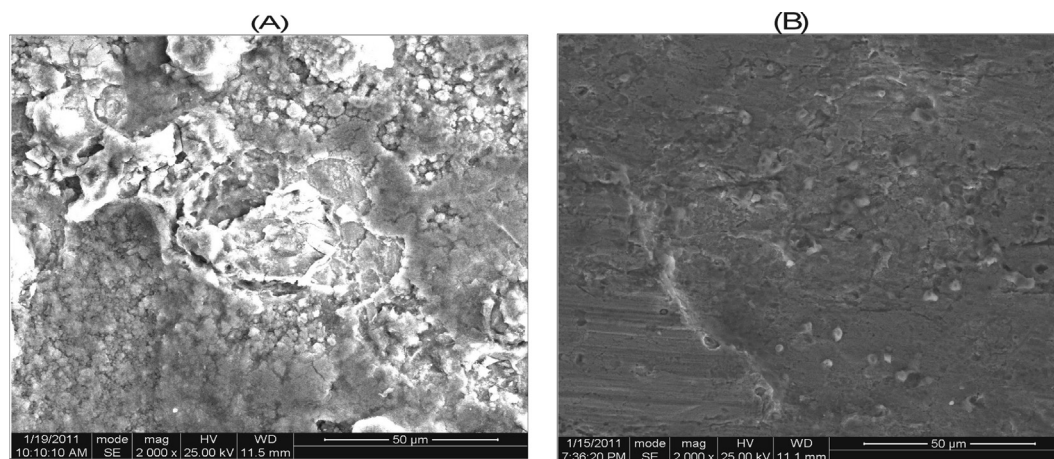
Gas chromatography (GC)-mass spectroscopy (MS) analysis of MO leaf extract from ethanol revealed the presence of 29 different compounds (Fig. 10). Table 5 contains some of the identified individual compounds. The compounds with less than 2% peak area were left out because of space. Structural assignment GC retention data of compounds is based on spectral matching with NIST library (National institute of Standards and Technology) (Ostovari et al., 2009).

### 3.6. Computational and theoretical considerations

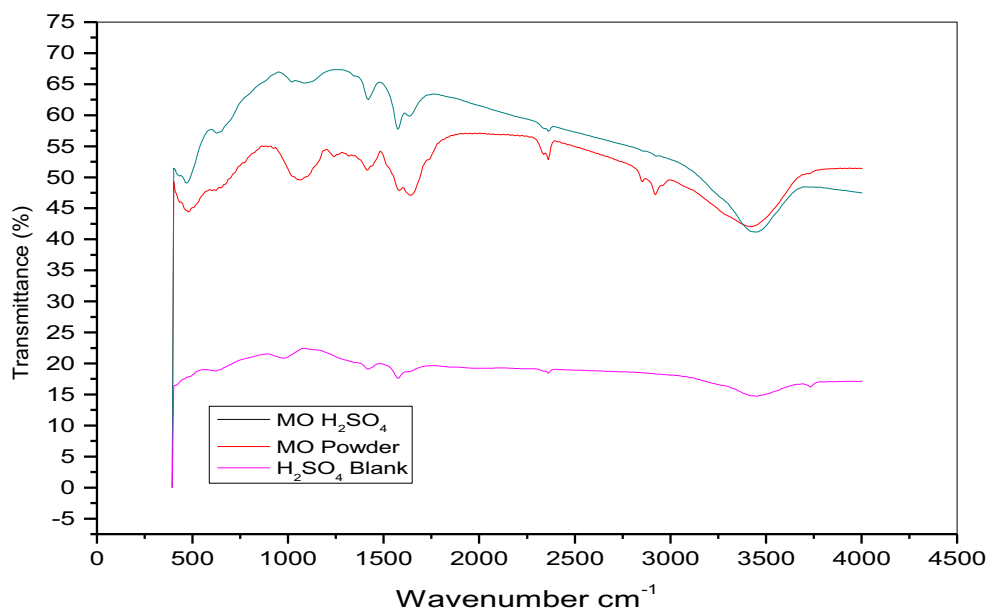
The effectiveness of an inhibitor can be related to its spatial molecular structure, as well as with their molecular electronic structure (Al-Sabgh et al., 2013). The present work was therefore extended to establish the effectiveness of some of the extract constituents as corrosion inhibitors using the tools of density functional theory. Plant extracts mass as usually obtained is a complex mix of different substance which make

Table 4 Impedance parameters of mild steel in 0.5 M  $\text{H}_2\text{SO}_4$  at 303 K in the absence and presence 1.5 g/L MO extract (ethanol and water extracts).

System	$R_s$ ( $\Omega \text{ cm}^2$ )	$R_{ct}$ ( $\Omega \text{ cm}^2$ )	$C_{dl}$ ( $\mu\text{F cm}^{-2}$ )	$n$	$\eta$ (%)
0.5 M $\text{H}_2\text{SO}_4$	1.689	119.7	504.0	0.7865	–
1.5 g/l Ethanol extract	1.289	367.6	196.5	0.7701	67.43
1.5 g/l Water extract	1.965	299.8	111.6	0.8778	60.07



**Fig. 8** SEM micrograph of mild steel after immersion in 0.5 M  $\text{H}_2\text{SO}_4$  for 24 h without and with MO extract at 303 K (a and b respectively).



**Fig. 9** FTIR spectra of mild steel surface in 0.5 M  $\text{H}_2\text{SO}_4$  at 303 K in the absence and presence of 1.5 g/L of MO extract.

it difficult to assess each component singly. Fig. 11 represents the structures selected for investigation. The basis of selection is related to percentage composition as well as structural differences. Thus, DFT calculations were performed, and the optimized geometry structures and the frontier molecular density distribution of the inhibitors are presented in Fig. 12. Table 6 collects some of the key quantum chemical parameters often used to gauge the efficiency of a molecule such as highest occupied molecular energies ( $E_{\text{HOMO}}$ ), lowest unoccupied molecular energies  $E_{\text{LUMO}}$ , energy gap ( $\Delta E$ ), etc., though detailed description of them is not intended in this study. However, there is a common belief in the literature that the higher the value of  $E_{\text{HOMO}}$  of the inhibitor, the greater is the ease of the inhibitor to offer electrons to the unoccupied d orbital of metal atoms, and higher the inhibition efficiency (Ma, 2006). Further lower the  $E_{\text{LUMO}}$ , the easier the acceptance of electrons from the metal atom to form feedback bonds. Another

parameter always given due mention is the gap energy ( $E_{\text{LUMO}}-E_{\text{HOMO}}$ ) of the molecule. The smaller the value of  $\Delta E$  of an inhibitor, the higher is the inhibition efficiency of that inhibitor (Issa et al., 2008). According to the work of Issa et al., (2008), a low  $\Delta E$  facilitates adsorption of the molecule and thus will cause higher inhibition efficiency. There was no particular trend in properties assessed, but since the compounds are from the same source, it is likely they complement each other. As Fig. 11 shows, the distributions of HOMO and LUMO for BANH and FCDH were on the benzene and furan rings respectively. Because of aromaticity the molecules are flat and lack discrete double bonds. This kind of distribution favor the preferential adsorption of aromatic rings on the metal surface (Zhang et al., 2010). For NHDA the distribution on were on the heteroatoms. The double bonds at positions 9 and 12 on ODDA were the HOMO location. Consequently these are the favorite sites for interaction with metal surface (see Fig. 13).

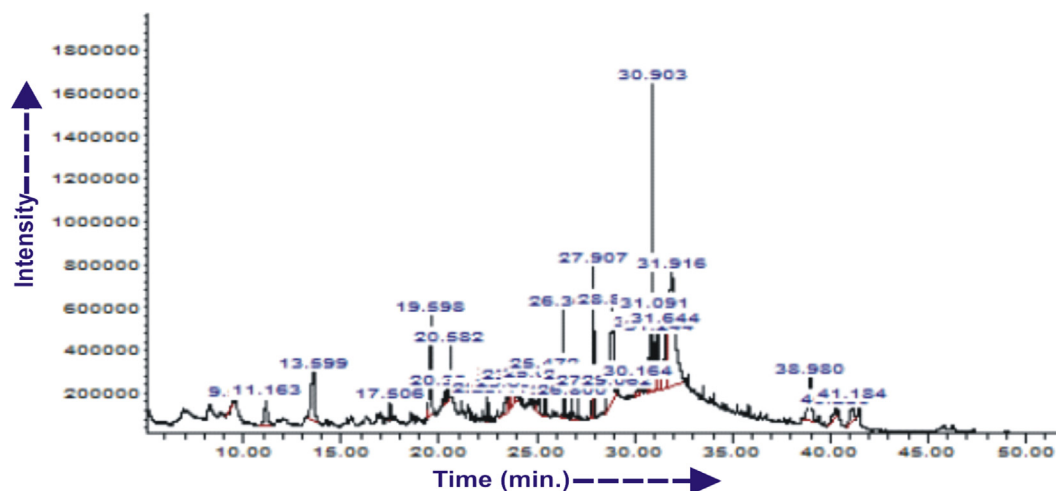


Fig. 10 GC/MS Chromatogram for the ethanol extract of M.O leaves.

**Table 5** Gas chromatography (GC)-mass spectroscopy (MS) data of MO leaves extract.

Retention time (min)	Compounds	Molecular Formula	Molecular Weight	Peak Area %
11.164	4H-Pyran-4-one, 2,3-dihydro-3,5-dihydroxy-6-methyl-	C <sub>6</sub> H <sub>8</sub> O <sub>4</sub>	144.12532	2.59
13.601	2-Furancarboxaldehyde, 5-(hydroxymethyl)-	C <sub>6</sub> H <sub>6</sub> O <sub>3</sub>	126.1100	5.60
19.598	Benzene acetonitrile, 4-hydroxy	C <sub>8</sub> H <sub>7</sub> NO	133.1473	6.31
33.655	2,4,4-Trimethyl-1-hexene	C <sub>9</sub> H <sub>12</sub>	126.24	3.66
26.361	Bicyclo[3.1.1]heptane, 2,6,6-trimethyl-, (1 $\alpha$ ,2 $\beta$ ,5 $\alpha$ )-	C <sub>10</sub> H <sub>18</sub>	138.24992	2.31
27.906	Hexadecanoic acid, methyl ester	C <sub>17</sub> H <sub>34</sub> O <sub>2</sub>	270.4507	3.49
28.896	n-Hexadecanoic acid	C <sub>16</sub> H <sub>32</sub> O <sub>2</sub>	256.4241	11.24
30.904	9,12,15-Octadecatrienoic acid, methyl ester	C <sub>19</sub> H <sub>32</sub> O <sub>2</sub>	292.4562	9.31
31.093	Phytol	C <sub>20</sub> H <sub>40</sub> O	292.4562	2.92
31.642	(Z,Z)-9,12-Octadecadienoic acid	C <sub>18</sub> H <sub>36</sub> O	296.4720	28.55
38.978	Heptadecane	C <sub>17</sub> H <sub>36</sub>	240.47	4.85
41.181	1-Methyl-4-(trimethylsilyl)-5-(isopropylcarbamoyloxy)-1H-indole	C <sub>16</sub> H <sub>24</sub> N <sub>2</sub> O <sub>2</sub> Si	304.459503	2.18

Furthermore, MD simulation was implemented to get additional evidence about the interaction between inhibitor molecule and metal surface. We have ensured that the whole system reached equilibrium until both temperature and energy were balanced. The equilibrium configuration (top and side views) of Fe(1 1 0) adsorption system is shown in Fig. 12. It clear from Fig. 12 that BANH and FCDH adsorbed parallel on the metal surface despite initial configuration of these molecules (perpendicular, tilt and parallel considered). Regarding NHDA and ODDA, it was the head groups of the molecules that were preferentially adsorbed on the metal surface because of strong charge transfer effect, which was in accordance with the analysis of distribution of HOMO and LUMO mentioned above. The adsorption energy of inhibitors on metal surface was an important criterion to judge its inhibition performance. It is generally assumed that a negative  $E_{ads}$  value suggests a stronger interaction between the adsorbent and the adsorbate. In this work, the calculated  $E_{ads}$  values ( $-64.86$ ;  $-69.75$ ;  $-166.4$ – $184.7$  kJ mol<sup>-1</sup> for BANH, FCDH, NHDA and ODDMA respectively. Therefore spontaneous adsorption can be expected (Tan et al., 2020).

### 3.7. Proposed mechanism of inhibition

It has been assume that organic molecules establish their inhibition action via adsorption of the inhibitor atom unto the metal surface (Isa et al., 2006). In general two modes of adsorption are applicable; chemical adsorption and physical adsorption. The presence of a transitional metal having vacant orbital of low energy with inhibitor molecule having relative loosely bound electrons or heteroatoms with lone pair of electrons facilitate chemical adsorption. However, small adsorption energies as obtained in this study, will indicate physical adsorption due to weak van der Waals interaction between the inhibitor and the metal surface. This result collaborates our earlier observations in Section 3.1.3.

## 4. Conclusion

The inhibition and adsorption behavior of MO leaves extract with ethanol for mild steel corrosion in 0.5 M H<sub>2</sub>SO<sub>4</sub> has been fully investigated.

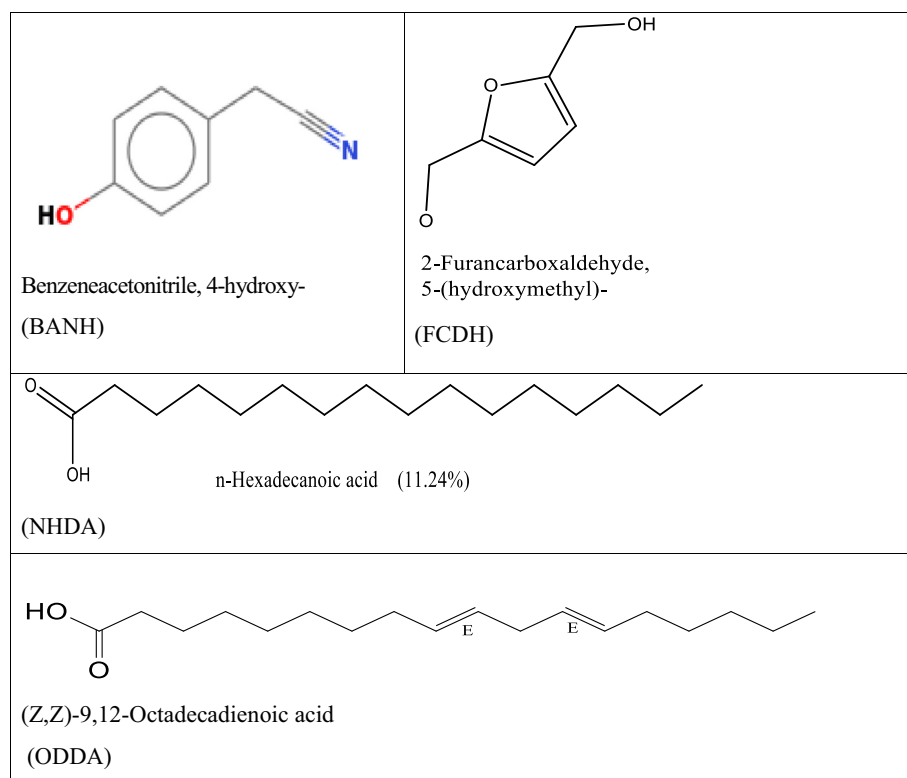


**Fig. 11** The molecular structures of plant extract composition, selected for DFT investigation.

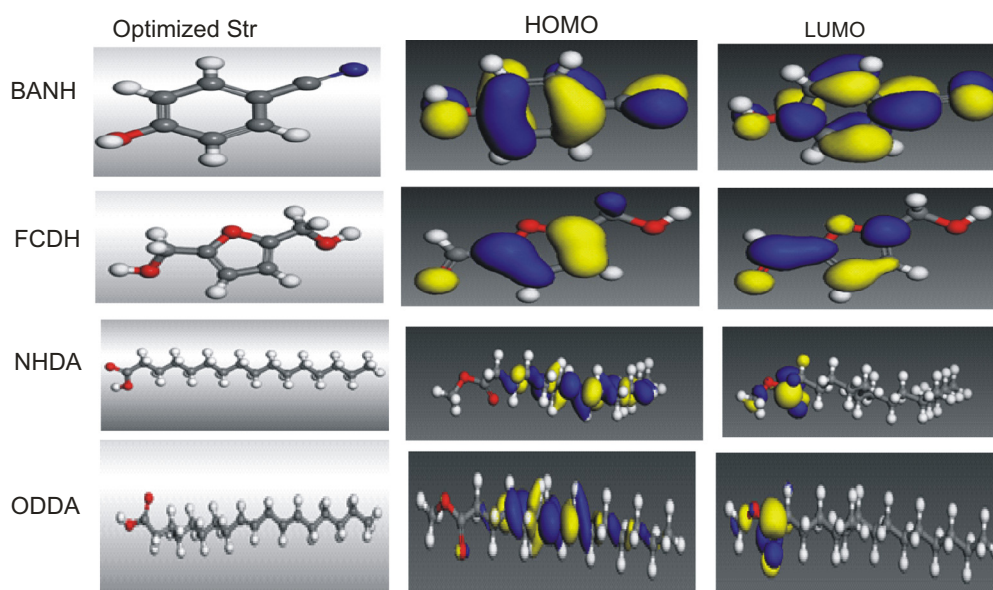


**Fig. 12** The optimized geometry structures and the frontier molecular density distribution of the inhibitors (Legend: White = Hydrogen; Grey = Carbon; Blue = Nitrogen; Red = Oxygen).

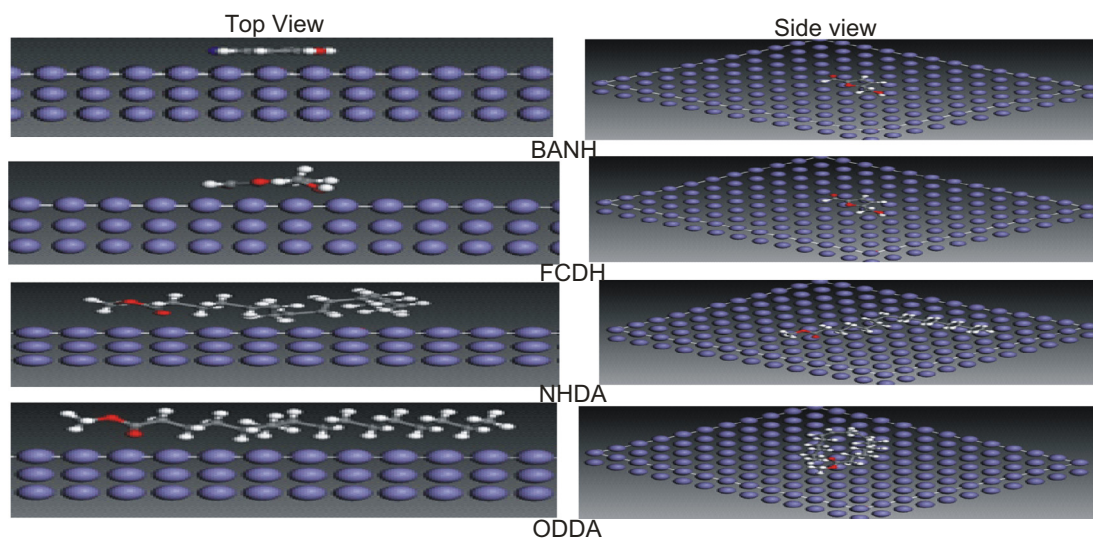
The inhibition efficiency was found to be concentration dependent reaching to 94.0% at 1.5 g/L and 303 K for 24 h but decreased with rising temperature and extended immersion time. Potentiodynamic polarization measurements showed that the additives act as mixed type inhibitors. The Langmuir isotherm best fits the data obtained and suggests physical

adsorption as the adsorption mechanism between the extract and the mild steel substrate.

The GC-MS spectrum shows presence of haloalkane, plant acids, alkanol, esters, aldehydes and ketones. The quantum chemical analysis revealed that the reactive sites of the select compounds (BANH and FCDH) are located at aromatic ring,

**Table 6** Some calculated quantum chemical parameters.

Property	BANH	FCDH	NHDA	ODDA
$E_{\text{HOMO}}$ (eV)	-9.512	-8.828	-9.915	-8.398
$E_{\text{LUMO}}$ (eV)	-0.378	-1.287	-0.445	-0.285
$E_{\text{LUMO}}-E_{\text{HOMO}}$ ( $\Delta E$ )	9.134	7.541	9.47	8.113
Mol. Surf. Area ( $\text{\AA}^2$ )	143.211	159.237	401.066	434.321
Bind. Energy (Kcal/mol)	-64.86	-69.75	-166.4	-184.7

**Fig. 13** The equilibrium configuration (top and side views) of studied structures adsorption models on Fe(1 1 0).

and these molecules can form coordinate and back-donating bonds with atoms on metal surface.

The result of molecular dynamics simulation demonstrate that the adsorption energy increased with the elongation of alky chain, which implied that the combination between the inhibitor molecule and metal surface enhanced. Quantum chemical methods can be an effective tool for assessing inhibitor performance.

#### Declaration of Competing Interest

The authors declare that they have no known competing financial interests or personal relationships that could have appeared to influence the work reported in this paper.

#### Acknowledgements

Support from the World Bank Africa Centers of Excellence for Impact (Ace Impact) project (NUC/ES/507/1/304) is greatly acknowledged.

#### References

Abdallah, M., 2002. Rhodanine azosulpha drugs as corrosion inhibitors for corrosion of 304 stainless steel in hydrochloric acid solution. *Corros. Sci.* 44, 717–728.

Abdel Gaber, A.M., Rahal, H.T., Beqai, F.T., 2020. *Eucalyptus* leaf extract as a eco-friendly corrosion inhibitor for mild steel in sulfuric and phosphoric acid solutions. *Int. J. Indus. Chem.* <https://doi.org/10.1007/s40090-020-00207-z>.

Abd El Rehim, S.S., Ibrahim, M.A.M., Khalid, K.F., 2001. The inhibition of 4-(20-amino-50 – methylphenylazo) antipyrine on corrosion of mild steel in HCl solution. *Mater. Chem. Phys.* 70, 268–273.

Abd El-Maksoud, S.A., Fouda, A.S., 2005. some pyridine derivatives as corrosion inhibitors for carbon steel in acidic medium. *Mater. Chem. Phys.* 93, 84–90.

Abdu, N.J.A., Sathiq, A.M., 2016. N- [Morpholin-4-yl (phenyl) methyl] acetamide as corrosion inhibitor for mild steel in hydrochloric acid medium. *Arab. J. Chem.* 9, S691–S698.

Akalezi, C.O., Emeka, E., Oguzie, E.E., 2016a. Evaluation of anticorrosion properties of Chrysophyllum albidum leaves extract for mild steel protection in acidic media. *Int. J. Ind. Chem.* 7, 81–92. <https://doi.org/10.1007/s40090-015-0057-5>.

Akalezi, C.O., Ogukwe, C.E., Ejele, E.A., Oguzie, E.E., 2016b. Mild steel protection in acidic media using *Mucuna pruriens* seed Extract. *Int. J. Corros. Scale Inhib.* 5 (2), 132–146.

Allaoui, M., Rahim, O., Sekhri, L., 2017. Electrochemical study on corrosion inhibition of iron in acidic medium by *Moringa oleifera* extract. *Oriental J. Chem.* 33 (2), 637–646.

Al-Sabgh, A.M., Notaila, M.N., Ahmed, A.F., Mohamed, A.M., Abdulmonem, M.F.E., Tahany, M.N., 2013. Structure effect of some amine derivatives on corrosion inhibition efficiency for carbon steel in acidic media using electrochemical and Quantum

- Theory Methods. *Egyptian Journal of Petroleum* 22 (1), 101–116. <https://doi.org/10.1016/j.ejpe.2012.09.004>.
- Al-Turkustani, A.M., Arab, S.T., Al-Qarni, L.S.S., 2011. Medicago Sativa plant as safe inhibitor on the corrosion of steel in 2.0M H<sub>2</sub>SO<sub>4</sub> solution. *J. Saudi Chem. Soc.* 15 (1), 73–82.
- Antonijevic, M.M., Milic, S.M., Petrovic, M.B., 2009. Films formed on copper surface in chloride media in the presence of azoles. *Corros. Sci.* 51 (6), 1228–1237.
- Anwar, F., Bhang, M.I., 2003. Analytical characterization of *Moringa oleifera* seed oil grown in temperate regions of Pakistan. *J. Agric. Food Chem.* 51, 6558–6563.
- Arabshahi, D.S., Devi, D.V., Urooj, A., 2007. Evaluation of antioxidant activity of some plant extracts and their heat, pH and storage stability. *Food Chem.* 100, 1100–1105.
- Bothi, Raja, Mathur, G.S., 2009. Solanum Tuberosum as an Inhibitor of Mild Steel Corrosion in Acid Media. *IJJAC* 28 (1), 77–84.
- Cruz, J., Martínez-Palou, R., Genesca, J., García-Ochoa, E., 2004. Experimental and theoretical study of 1-(2-ethylamino)-2-methylimidazole as an inhibitor of carbon steel corrosion in acid media. *J. Electroanal. Chem.* 566 (1), 111–121.
- Das, M., Biswas, A., Kundu, B.K., Mobin, S.M., Udayabhanub, G., Mukhopadhyay, S., 2017. Targeted synthesis of cadmium(II) Schiff base complexes towards corrosion inhibition on mild steel. *RSC Adv.* 7, 48569.
- El-Haddad, M.N., Elattar, K.M., 2015. Synthesis, characterization and inhibition effect of new antipyrinyl derivatives on mild steel corrosion in acidic solution. *Int. J. Ind. Chem.* 6, 105–117.
- El-Etre, A.Y., Abdallah, M., El-Tantawy, Z.E., 2005. Corrosion inhibition of some metals using lawsonia extract. *Corros. Sci.* 47 (2), 385–395.
- Ergun, Ü., Yüzer, D., Emregül, K.C., 2008. The inhibitory effect of bis-2,6-(3,5-dimethylpyrazolyl) pyridine on the corrosion behaviour of mild steel in HCl solution. *Mater. Chem. Phys.* 109, 492–499.
- Hosseini, M., Mertens, S.F.L., Ghorbani, M., Arshadi, M.R., 2003. *Mater. Chem. Phys.* 78, 800–808. [https://doi.org/10.1016/S0254-0584\(02\)00390-5](https://doi.org/10.1016/S0254-0584(02)00390-5).
- Hussin, M.H., Jain Kassim, M., Razali, N.N., Dahon, N.H., Nasshorudin, D., 2016. *Arab. J. Chem.* 9, S616–S624.
- Issa, R.M., Awad, M.K., Atlam, F.M., 2008. Quantum chemical studies on the inhibition of corrosion of copper surface by substituted uracils. *Appl. Surf. Sci.* 255, 2433.
- Issaadi, S., Douadi, T., Zouaoui, A., Chafaa, S., Khan, M.A., Bouet, G., 2011. Novel thiophene symmetrical Schiff base compounds as corrosion inhibitor for mild steel in acidic media. *Corros. Sci.* 53, 1484–1488. <https://doi.org/10.1016/j.corsci.2011.01.022>.
- Jalajaa, D., Jyothi, S., Muruganantham, V.R., Mallik, J., 2019. *Moringa oleifera* gum exudate as corrosion inhibitor on mild steel in acidic medium, *Rasāyan, Chem.* 12(2), 545–548.
- Jeetendra Bhawsar, Jain, P.K., Preeti Jain, 2015. Experimental and computational studies of *Nicotiana tabacum* leaves extract as green corrosion inhibitor for mild steel in acidic medium. *Alexandria Eng. J.* 54(3), 769–775.
- Jones, D.A., 1983. *Principles and Prevention of Corrosion*. Prentice Hall, Upper Saddle River, NJ.
- Khaled, K., 2003. F (2003), The inhibition of benzimidazole derivatives on corrosion of iron in 1 M HCl Solutions. *Electrochim. Acta* 48, 2493.
- Khaled, K.F., Babi, K., Hackerman, N., 2004. Piperidines as corrosion inhibitors for iron in hydrochloric acid. *Electrochim. Acta* 485–495. <https://doi.org/10.1016/j.electacta.2003>.
- Kumar, P., Mohana, K.N., 2013. The Effect of *Achyranthes Aspera* Extracts on Mild Steel Corrosion in Industrial Water Medium, Hindawi Publishing Corporation, ISRN Corrosion, ID 261847.
- Li, X., Deng, S., Fu, H., 2011. Triazolyl blue tetrazolium bromide as a novel corrosion inhibitor for steel in HCl and H<sub>2</sub>SO<sub>4</sub> solutions. *Corros. Sci.* 53, 302–309. <https://doi.org/10.1016/j.corsci.2010.09.036>.
- Likhanova, N.V., Martínez-Palou, R., Veloz, M.A., Matias, D.J., Reyes-Cruz, V.E., Olivares-, Xometl O., 2007. Microwave-assisted synthesis of 2-(2-pyridyl) azoles. Study of their corrosion inhibiting properties. *J. Heterocyclic Chem.* 44 (1), 145–153.
- Liu, F.G., Du, M., Zhang, J., Qiu, M., 2009. Electrochemical behavior of Q235 steel in saltwater saturated with carbon dioxide based on new imidazole derivative inhibitor. *Corros Sci* 51 (1), 102–109.
- Ma, H., Chen, S., Liu, Z., Sun, Y., 2006. Theoretical elucidation on the inhibition mechanism of pyridine-pyrazole compound: a Hartree Fock study. *J. Mol. Struct.: Theochem.* 774, 19–22.
- Martinez-Palou, R., Rivera, J., Zepeda, L.G., Rodríguez, A.N., Hernandez, M.A., Marín-Cruz, J., Estrada, A., 2004. Evaluation of corrosion inhibitors synthesized from fatty acids and fatty alcohols isolated from sugar cane wax. *Corrosion* 60 (5), 465–470.
- Martinez, S., 2003. Inhibitory mechanism of mimosa tannin using molecular modeling and substitution adsorption isotherms. *Mater. Chem. Phys.* 77, 97–102.
- Morad, M.S., 2000. An electrochemical study on the inhibiting action of some organic phosphonium compounds on the corrosion of mild steel in aerated acid solutions. *Corros. Sci.* 42, 1307.
- Nadkarni, K.M., 2009. *Indian material medica*. Bombay Popular Prakashan, 811–816.
- Nahle, A., El-Hajjaji, F., Ghazoui, A., Benchat, N.E., Taleb, M., Saddik, R., Hammouti, B., 2018. Effect of substituted methyl group by phenyl group in pyridazine ring on the corrosion inhibition of mild steel in 1.0 M HCl. *Anti-Corros. Method* 65, 87–96.
- Nam, N., Bui, C.V., Mathesh, M., Tan, Y.J., Forsyth, M., . A study of 4-carboxyphenylboronic acid as a corrosion inhibitor for steel in carbon dioxide containing environments. *Corros. Sci.* 76, 257–266.
- Noor, E.A., 2007. Temperature effects on the corrosion inhibition of mild steel in acidic solutions by aqueous extract of fenugreek leaves. *Int. J. Electrochem. Sci.* 2, 996–1017.
- Popova, A., Christov, M., Zvetanova, A., 2007. Effect of the molecular structure on the inhibitor properties of azoles on mild steel corrosion in 1 M hydrochloric acid. *Corros. Sci.* 49 (5), 2131–2143.
- Okafor, P.C., Ebenso, E.E., Ekpe, U.J., 2010. *Azadirachta indica* extracts as corrosion inhibitor for mild steel in acid medium. *Int. J. Electrochem. Sci.* 5 (7), 978–993.
- Noor, EA, 2009. Noor EA. Evaluation of inhibitive action of some quaternary N-heterocyclic compounds on the corrosion of Al–Cu alloy in hydrochloric acid. *Material Chemistry Physics* 114, 533–541.
- Oguzie, E.E., Enenebeaku, C.K., Akalezi, C.O., Okoro, S.C., Ayuk, A. A., Ejike, E.N., 2012. adsorption and corrosion-inhibiting effect of *Dacryodis edulis* extract on low-carbon-steel corrosion in acidic media. *J. Colloid Interface Sci.* 349 (1), 283–292.
- Olivares-Xometl, O., Likhanova, N.V., Domínguez-Aguilar, M.A., Arce, E., Dorante, H., Arellanes-Lozada, P., 2008. Synthesis and corrosion inhibition of alpha-amino acids alkylamides for mild steel in acidic environment. *Mater. Chem. Phys.* 110 (2–3), 344–351.
- Olivares-Xometl, O., Likhanova, N.V., Gómez, B., Navarrete, J., Llanos-Serrano, M.E., Arce, E., Hallen, J.M., 2006. Electrochemical and XPS studies of decylamides of alpha-amino acids adsorption on carbon steel in acidic environment. *Appl. Surf. Sci.* 252 (6), 2894–2909.
- Olivares-Xometl, O., Likhanova, N.V., Martínez-Palou, R., Domínguez-Aguilar, M.A., 2009b. (2009), Electrochemistry and XPS study of an imidazole as corrosion inhibitor of mild steel in acidic environment. *Mater. Corros.* 60 (1), 14–21.
- Ostovari, A., Hoseinie, S.M., Peikari, M., Shadizadeh, S.R., Hashemi, S.J., 2009. Corrosion inhibition of mild steel in 1 M HCl solution by henna extract: a comparative study of the inhibition by henna and its constituents (Lawson, gallic acid, a-D-glucose and tannic acid). *Corros. Sci.* 51, 1935–1949.

- Popova, A., Sokolova, E., Rlicheva, S., Christov, M., 2003. AC and DC study of the temperature effect on mild steel corrosion in acid media in the presence of benzimidazole derivatives. *Corros. Sci.* 45 (1), 33–58.
- Ramachandran, C., Peter, K.V., Gopalakrishna, P.K., 1980. Drumstick (*Moringa oleifera*)- a multipurpose Indian vegetable. *Econ. Bot.* 34, 276–283.
- Roque, J.M., Pandiyan, T., Cruz, J., Garcia-Ochoa, E., 2008. DFT and electrochemical studies of tris(benzimidazole-2-ylmethyl)amine as an efficient corrosion inhibitor for carbon steel surface. *Corros. Sci.* 50 (2008), 614–624.
- Sastri, V.S., 1998a. *Green Corrosion Inhibitors-Theory and Practice*. John Wiley and Sons, Hoboken, NJ.
- Sastri, V.S., 1998b. *Corrosion Inhibitors Principles and Applications*. John Wiley and Sons, New York.
- Satapathy, A.K., Gunasekaran, G., Sahoo, S.C., Amit, K., Rodrigues, P.V., 2009. Corrosion inhibition by *Justicia gendarussa* plant extract in hydrochloric acid solution. *Corros. Sci.* 51, 2848–2856. <https://doi.org/10.1016/j.corsci.2009.08.016>.
- Shalabi, K., Abdallah, Y.M., Hassan, H.M., Fouda, A.S., 2014. Adsorption and corrosion inhibition of *Atropa Belladonna* extract on carbon steel in 1 M HCl solution. *Int. J. Electrochem. Sci.* 9, 1468–1487.
- Singh, A., Ebenso, E.E., Quraishi, M.A., 2012a. Corrosion inhibition of carbon steel in HCl solution by some plant extracts. *Int. J. Corros.* <https://doi.org/10.1155/2012/897430>.
- Singh, A., Ahamad, I., Yadav, D.K., Singh, V.K., Quraishi, M.A., 2012b. The effect of environmentally benign fruit extract of Shahjan (*Moringa oleifera*) on the corrosion of mild steel in hydrochloric acid solution. *Chem. Eng. Comm.* 199, 63–77.
- Singh, A., Talha, M., Xu, X., Sun, Z., Lin, Y., 2017. Heterocyclic corrosion inhibitors for J55 Steel in a sweet corrosive medium. *ACS Omega* 2, 8177–8186.
- Solmaz, R., Kardas, G., Culha, M., Yazici, B., Erbil, M., 2008. Investigation of adsorption and inhibitive effect of 2-mercaptothiazoline on corrosion of mild steel in hydrochloric acid media. *Electrochim. Acta* 53, 5941–5952. <https://doi.org/10.1016/j.electacta.2008.03.055>.
- Szauer, T., Brandt, 1981. Adsorption of oleates of various amines on iron in acidic solution. *Electrochim Acta* 26, 1253–1256.
- Tan, J., Guo, L., Yang, H., Zhang, F., El Bakri, Y., 2020. Synergistic effect of potassium iodide and sodium dodecyl sulfonate on the corrosion inhibition of carbon steel in HCl medium: a combined experimental and theoretical investigation. *RSC Adv.* 10, 15163–15170.
- Vasudha, V.G., Priya, S.K., 2012. *Polyalthia longifolia* as a corrosion inhibitor for mild steel in HCl solution. *Res. J. Chem. Sci.* 3 (1), 21–26.
- Zhang, J., Liu, J., Yu, W., Yan, Y., You, L., Liu, L., 2010. Molecular modeling of the inhibition mechanism of 1-(2-aminoethyl)-2-alkylimidazoline. *Corros. Sci.* 52, 2059–2065.
- Zarrouk, A., Hammouti, B., Lakhlifi, T., Traisnel, M., Vezin, H., Bentiss, F., 2015. (2015), New 1*H*-pyrrole-2,5-dione derivatives as efficient organic inhibitors of carbon steel corrosion in hydrochloric acid medium: electrochemical, XPS and DFT studies. *Corros. Sci.* 90, 572–584.